

Basic Research Grants Scheme 2002

A Study of Damage Initiation and Growth in Composite Bolted Joints

Project N°: SC/02/191

Deliverable No: D1.1

Review of Failure and Damage Models for Composite Bolted Joints

Michael McCarthy, Gouri Padhi, Conor McCarthy

*Department of Mechanical and Aeronautical Engineering
University of Limerick
Limerick
Ireland*



University of Limerick

Contents

| | | |
|---|--|----|
| 1 | Introduction | 3 |
| 2 | Overview of Composite Bolted Joint Design | 4 |
| | 2.1 Bearing Failure | 7 |
| | 2.2 Net-tension Failure | 7 |
| | 2.3 Shear-out Failure | 8 |
| | 2.4 Cleavage Failure | 8 |
| | 2.5 Fastener Pull-through | 8 |
| | 2.6 Bolt Failure | 9 |
| 3 | Progressive Damage Analysis of Composite Bolted Joints | 10 |
| | 3.1 Introduction to Progressive Damage Methodology | 10 |
| | 3.2 Failure Criteria | 11 |
| | 3.3 Non-linear Shear Behaviour | 13 |
| | 3.4 Degradation Rules | 13 |
| 4 | Continuum Damage Mechanics | 16 |
| | 4.1 Allen's model | 16 |
| | 4.2 Ladeveze's model | 17 |
| | 4.3 Talreja's CDM model | 18 |
| | 4.4 Plasticity based CDM model | 19 |
| 5 | Conclusions | 21 |
| | Acknowledgements | 22 |
| | References | 23 |

Section 1: Introduction

The project “A Study of Damage Initiation and Growth in Composite Bolted Joints” is funded under the Basic Research Grants Scheme 2002, jointly administered by Enterprise Ireland and the Irish Research Council for Science, Engineering and Technology. It runs from October 2002 to September 2005.

The goal of the project is to develop computational models for prediction of the initiation and growth of damage in composite bolted joints. Two approaches will be investigated. The first will be based on a stiffness reduction scheme. The second will be based on continuum damage mechanics. The two approaches will be compared against experimental data generated within the project and also from a previous EU research project, and critically assessed.

In this first deliverable of the modelling part of the project, a review is presented of failure and damage models used to date for composite bolted joints. The review begins with an overview of composite bolted joint design practice, and a discussion of the different kinds of failure modes which occur. Next a discussion of various methods used to date (all using stiffness reduction schemes as opposed to continuum damage mechanics) to model damage progression in joints is given. Finally various continuum damage models which have been applied to e.g. centre-notched specimens and open-hole specimens (but not yet joints) are presented as it is planned to develop these and apply them to bolted joints in this project.

Section 2: Overview of Composite Bolted Joint Design

Composite bolted joint design has been and still is a major topic of research. The main driving force behind the use of composites for transport vehicles is the desire to reduce weight while maintaining safety. Efficient joint design is a critical aspect of maximising this weight saving. Considerable literature exists covering all aspects of composite joint design, including joint geometry, lay-up, clamp-up, friction, stress analysis, pin-lap joints, multi-bolt joints, failure mechanisms, delamination and progressive damage modelling, to name but a few. Excellent reviews on this topic have been given recently [1, 2]. The aim here is not to repeat the work of these authors, but to give a brief background to composite bolted joint design and the various failure modes which occur, and then proceed directly to the topic of interest, i.e. progressive damage analysis.

Aircraft structures contain a variety of bolted joint configurations, but despite this diversity, there is a basic commonality in the stresses set up by the bolt load at a particular hole and the effect of other loaded holes on this stress distribution [3]. This allows simplified coupon tests to be used in establishing design data for these various joint configurations. The intent is to then combine a suitable number of these test results to represent the actual situation. An example of reducing a complex primary structural joint down to a coupon test is shown in figure 2.1. Figure 2.1a shows a design of a hybrid composite-metal wing-box that was proposed in the EU project TANGO [4]. TANGO is a very large “Technology Platform” project led by Airbus, with the aim of developing and demonstrating alternative structural concepts (such as composite fuselage, composite wing etc.). Figure 2.1b shows a proposed hybrid metallic/composite wing together with a skin-stringer joint that could be used to connect the outer composite wing box to the inner metallic wing box of this structure. A representative “benchmark” for this type of joint was proposed by Airbus UK and is shown in figure 2.1c. Testing and analysis of this “benchmark” structure was carried out in the EU project BOJCAS [5] to gain an insight into its behaviour and failure mechanisms. To date, most research has been carried out at a coupon level on “benchmarks” similar to, but often simpler than that shown in figure 2.1c. Very little testing and analysis has been reported in the literature for actual aircraft joints which is probably due to the high costs associated with such work. The remainder of this section will therefore concentrate on reviewing previous work on composite joints analysed at a coupon level.

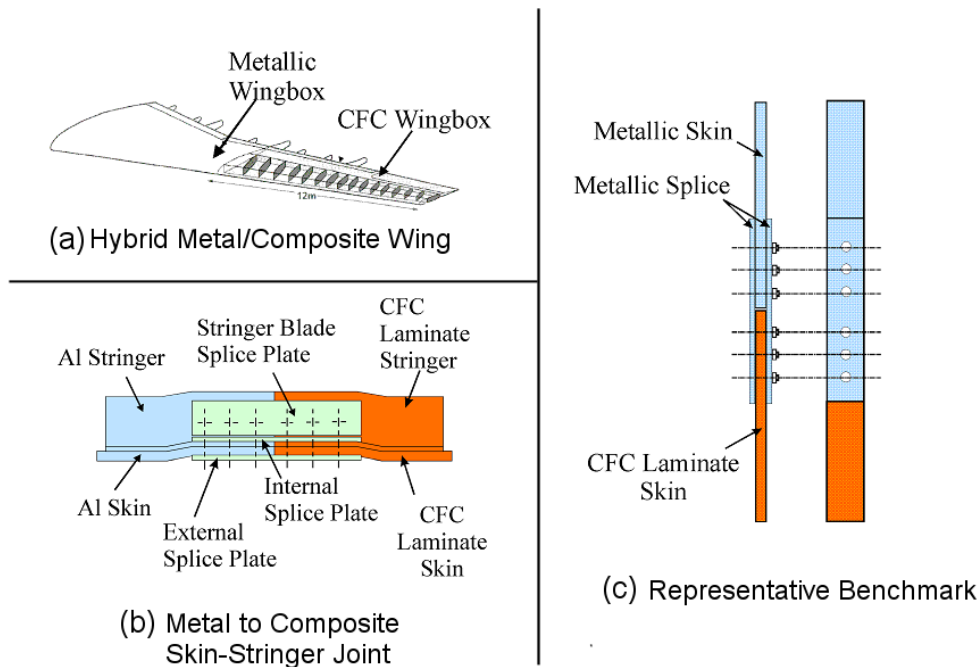
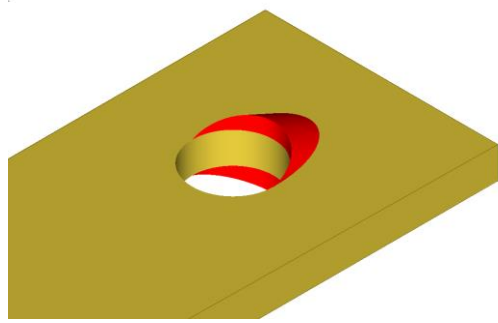


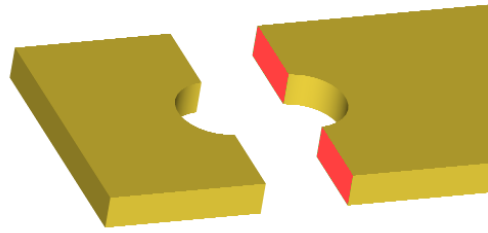
Figure 2.1 Metal to composite skin-stringer joint and proposed representative benchmark joint (courtesy Airbus UK)

The design of composite joints requires a sound understanding of the different failure modes. At a coupon level, there are generally six ways in which a composite bolted joint can fail. These modes are referred to as bearing, net-tension, shear-out, cleavage, fastener pull-through and bolt failure and are shown in figure 2.2a-2.2f respectively. Failure can also occur in more than one mode, either simultaneously or consecutively. The joint geometry predominantly controls the failure mode, however other factors such as material type, ply orientation, bolt-torque and loading configuration also contribute. Each failure mode results from quite different damage mechanisms occurring in the laminate and/or the bolt and are therefore discussed individually below.

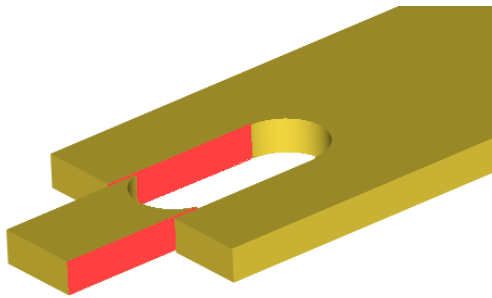
Before proceeding with the review, the terminology used here is discussed. Figure 2.3 shows an illustration of some common joint geometric parameters. The length, L , usually consists of two regions, the overlap region and the non-overlap region. The length of the overlap region is defined by the portion of the laminate that is in contact with another laminate. The length of non-overlap region is simply the remaining portion that is not in contact. The laminate contact interface is often referred to as the “shear plane”. The diameter, width, thickness and edge distance are defined as D , W , t and E respectively and are shown in figure 2.3. In the case of a multi-bolt joint, two additional parameters are used, viz. the distance (pitch) between bolt-hole centres along the loading direction, P_c (the column pitch), and transverse to the loading direction P_r (the row pitch). Generally, joints are characterised as single-lap or double-lap, as shown in figure 2.3. As will be seen in sections 2.1 - 2.4 failure modes are associated with failure planes and these planes are referred to as the bearing plane, the net-tension plane and the shear-out plane, highlighted in figure 2.3.



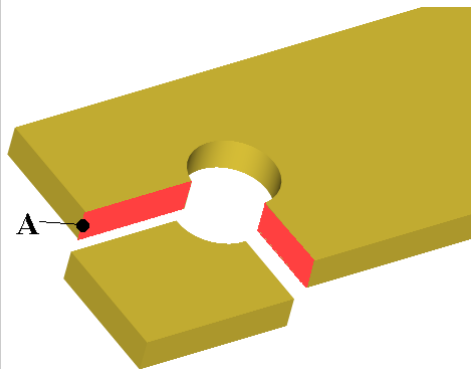
(a) Bearing Failure



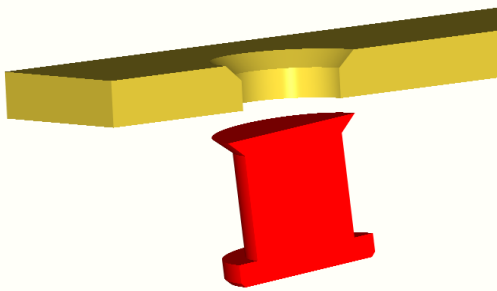
(b) Net Tension Failure



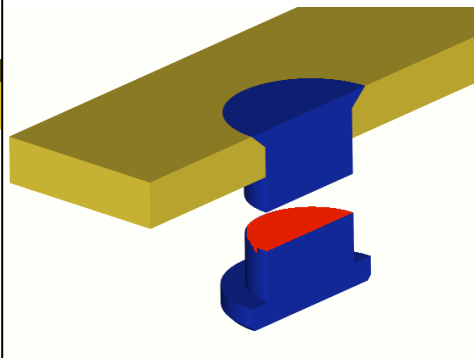
(c) Shear out failure



(d) Cleavage Failure



(e) Fastener Pull-through



(f) Bolt Failure

Figure 2.2 Failure Modes in Composite Bolted Joints

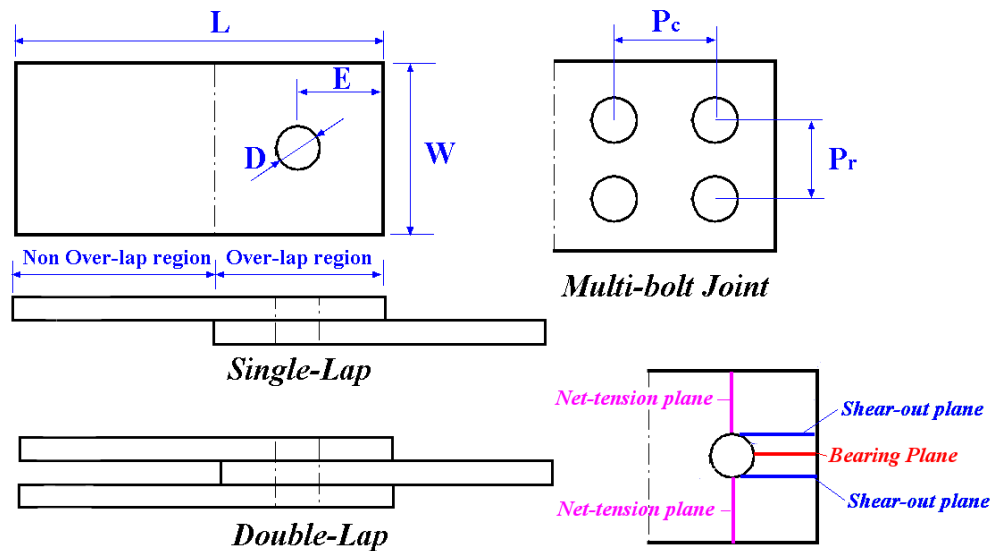


Figure 2.3 Definition of joint geometric parameters used in this thesis

2.1 Bearing failure

The bearing mode of failure is illustrated in figure 2.2a. It takes the form of a local crushing which occurs at the bolt-hole contact interface. The damaged material moves out-of-plane, causing considerable expansion in the thickness direction. Restricting this expansion by torquing the bolt can have a strong effect on this failure mode. In a single-bolt joint, this failure mode generally occurs when the ratio of width to bolt diameter (W/D) is large [3]. In a multi-bolt joint, it generally occurs at locations where the bolt row pitch to diameter ratio (P_r/D) is large [3] or where the ratio of by-pass load to bearing load is low [6] (by-pass load at a particular hole is basically the load which bypasses that hole and is transferred to the next hole). Bearing failure is the only non-catastrophic failure mode and is characterised by the accumulation of sub-critical damage mechanisms, beginning with matrix cracks, then related fibre micro-buckling and internal delamination, resulting in through thickness shear cracks that lead to final failure [7]. Wang et. al. [8] found that these damage mechanisms controlled bearing failure and that the final collapse occurred when damage propagated to a point where two shear cracks merged and initiated an unstable delamination growth or shear cracks reached the free surfaces of the laminate. Cooper & Turvey [9] stated that the bearing failure mode was normally desirable in composite bolted joints because it developed slowly, giving plenty of warning before ultimate failure.

2.2 Net-tension failure

The net-tension mode of failure is illustrated in figure 2.2b. This mode of failure occurs in single-bolt joints when the width to bolt diameter ratio (W/D) is small. For example, quasi-isotropic, graphite/epoxy laminates fail in this mode when $W/D < 4$, and glass/epoxy laminates fail when $W/D < 2$ [10]. In a multi-bolt joint, this failure mode occurs at locations where the bolt pitch to diameter ratio (P_r/D) is small [3] or where the ratio of by-pass load to bearing load is high [6]. As the bearing mode of failure is also related to the W/D ratio, there is a point where the failure mode changes from bearing to net-tension which happens with decreasing W/D , resulting in a loss of joint strength [11]. Camanho et al. [7] found that this

failure mode occurred catastrophically, without significant warning before final failure and that damage did not occur at the net section plane until 90% of the final failure load. At this load, they found delamination and matrix cracks which lead to a non-linearity in the load-displacement curve.

2.3 Shear-out failure

The shear-out mode of failure is illustrated in figure 2.2c. This mode of failure can be considered a special case of bearing failure and is frequently a consequence of bearing failure occurring in a joint with a short end distance. In fact, Kretsis & Matthews [11] found that as the end distance decreased the failure mode changed from bearing to shear-out, with a corresponding decrease in joint strength. However, this is not always the case as shear-out failures can occur in highly orthotropic laminates with very large end distances. Hart-Smith [10] found that shear-out failures are prevalent for fibre patterns that are both rich in 0° and deficient in 90° plies. With end-distance to diameter ratios (E/D) of 2 and 22, tests on boron-epoxy laminates with 50% 0° plies and 50% $\pm 45^\circ$ plies failed in the shear-out mode at the same load level. Camanho et al. [7] found this mode of failure to be catastrophic and the only warning before failure was noise emitted at 87% of the final failure load. The load-displacement curves from their tests were found to be linear until final failure. At 95% of the final failure load, fibre microbuckling and matrix cracks were present at the bearing plane and extensive matrix cracks and delamination were present on the shear-out plane.

2.4 Cleavage failure

The cleavage mode of failure is illustrated in figure 2.2d. This failure mode is often triggered from an incomplete net-tension failure and occurs in laminates with inadequate end distances and too few transverse (90°) plies. Hart-Smith [10] stated that this failure usually initiated at the end of the specimen (point A in figure 2.2d) rather than adjacent to the fastener. In contrast, Cooper & Turvey [9] stated that it initiated with longitudinal splitting of the laminate on the loaded side of the bolt, which caused the end of the joint to act as two cantilevers, causing large stress concentrations around the hole at the net-tension plane. These stress concentrations then promoted failure across the net-section of the joint, followed by final collapse. As with shear-out failures, this mode of failure can be avoided by optimally proportioned lay-ups [10].

2.5 Fastener pull-through

The fastener pull-through mode of failure is illustrated in figure 2.2e. This mode of failure mainly occurs in joints with countersunk head bolts. However, it does require sufficient laminate thickness to prevent it for all fastener arrangements. For any given geometry, this failure mode may vary as a function of the fibre pattern or lay-up sequence [10]. Chen & Lee [12] carried out a numerical and experimental study of a composite laminate loaded in the thickness direction by a countersunk fastener. Using progressive damage analysis with a three-dimensional finite element model, they found that the laminate sustained considerable damage and delamination as the fastener was pushed through.

2.6 Bolt failure

Bolt failure is illustrated in figure 2.2f. Although not a laminate failure, this failure mode is usually accompanied by considerable damage to the laminate. Lawlor et al. [13] found that considerable bearing damage occurred before bolt failure when testing single-lap, single-bolt composite joints and that final joint failure was through bolt failure. They also found that the bolt failed at the root of the thread where the minimum cross-sectional area was located.

Section 3: Progressive Damage Analysis of Composite Bolted Joints

A number of methods such as the point/average stress criterion, fracture mechanics and progressive damage models exist to predict the strength of composite bolted joints. The point stress and average stress criteria developed by Whitney & Nuismer [14] use stresses at a “characteristic distance” from a geometric discontinuity to predict failure and have been used by several investigators [15, 16, 17] for predicting bolted joint strength. The method however involves a high degree of empiricism and needs re-calibrating for each new material, lay-up etc. Fracture mechanics methods have been used by some authors [18] to predict joint strength but in general have found less acceptance in composite bolted joint design. Central to this investigation is progressive damage analysis (PDA) as it is the most promising method to predict the damage state in composite joints from only standard material test data. Progressive damage analysis and its application to bolted joints is thus discussed in this section.

3.1 Introduction to progressive damage methodology

A typical methodology for progressive damaging analysis (PDA) is shown in figure 3.1. This methodology has been described by many researchers [19, 20, 21] and the following description is common to all PDA found in the literature. Firstly a finite element model is constructed to represent the physical problem. Initial (un-damaged) material properties are assigned to the elements and the boundary conditions defined. At each load step, a non-linear analysis is performed until a converged solution is obtained. Assuming a converged solution is achieved, stresses and strains are recovered at all the Gauss points and used to evaluate the failure criteria employed. Once failure is detected at a particular Gauss point, the material properties are degraded according to the degradation law imposed. At this point, in the so-called “implicit” approach, equilibrium is re-established at the same load level because the initial non-linear solution no longer corresponds to the equilibrium state due to changes in material properties [21]. The iterative process of obtaining non-linear equilibrium solutions each time a local material property is changed is repeated until no additional lamina failures are detected. In contrast to this, some implementations of PDA omit the step of re-establishing equilibrium and this procedure is often referred to as an “explicit” implementation. In each approach, the load step is then incremented until catastrophic or global failure of the structure is detected.

For bolted joints applications, global failure in the form of net-tension and shear-out modes was determined by Camanho & Matthews [22] when the damage in the fibres extended to the laminate free edge. The authors stated that this would not work for bearing failure as the damaged region was contained within a small area beside the bolt-hole. Based on an approach by Hung & Chang [23], Camanho & Matthews [22] considered global bearing failure to have occurred when the damage reached the washer outer edge which was also based on experimental observation.

As shown in figure 3.1, a number of procedures are needed in order to carry out a progressive damage analysis. Procedures such as non-linear analysis to establish and re-establish equilibrium, and stress recovery are generally software dependent and therefore not discussed here. The main focus of this section is on failure criteria and property degradation rules used by previous researchers for progressive damage modelling of composite bolted joints.

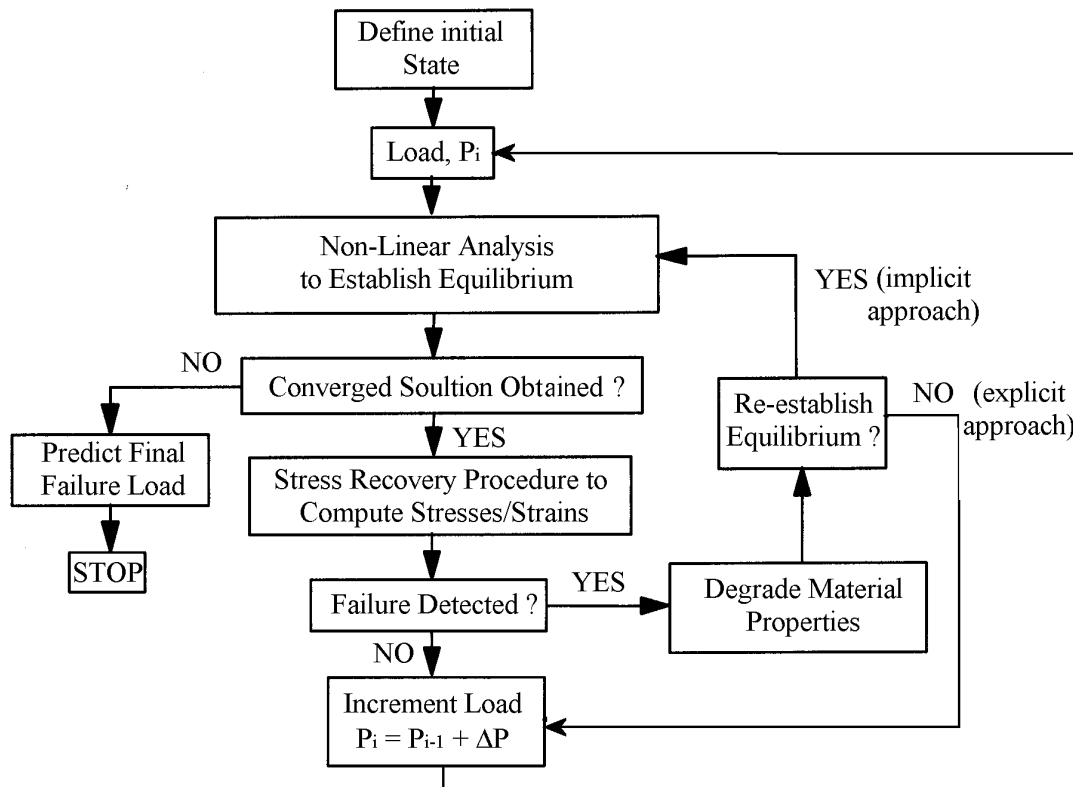


Figure 3.1 Progressive damage analysis procedure flow chart

3.2 Failure Criteria

Over thirty failure criteria exist for predicting strength of laminated composites and a comprehensive review of these theories was given by Nahas [24]. These theories generally fall into two categories, namely, interactive failure and independent failure. Interactive failure theories can only predict the onset of failure whereas independent failure theories can predict onset of failure as well as failure mode. Well known interactive theories are given by Hill [25] and Azzi-Tsai [26], but these theories do not account for different strengths in tension and compression which composites are known to exhibit. Interactive tensor polynomial theories such as that due to Tsai & Wu [27] use the concept of strength tensors, which allows for transformation from one coordinate system to another and accounting for different tensile and compressive strengths. A drawback with these theories is that they require biaxial test data which is difficult and expensive to determine [28].

Composite materials consist of mechanically dissimilar phases such as a compliant, yielding matrix and stiff elastic brittle fibres, which result in several different failure modes. Examples of such modes are fibres rupturing in tension or buckling in compression, matrix cracking and/or fibre matrix shearing. Other failure modes such as fibre matrix interface/interphase debonding also exist. These distinct failure modes can only be accounted for by independent failure criteria. Examples of the simplest independent failure criteria are the maximum stress and maximum strain failure criteria. These work by evaluating the stresses or strains in the principal material directions and comparing them against material allowables. Although simple in formulation, these theories can predict the failure mode. However they lack interaction terms with shear stresses, which makes them quite conservative [29]. To perform a

progressive failure analysis it is essential that the failure mode be known so that the appropriate material properties can be degraded. A well-known failure theory that has been used extensively in progressive failure analysis of bolted joints [19, 22, 29, 30, 31, 32, 33] was developed by Hashin [34]. Like the interactive tensor polynomial theories, the criteria are quadratic in stress space but can account for fibre and matrix failure in both tension and compression separately. The full three-dimensional form is listed below:

Tensile Matrix Mode, $\sigma_{22} + \sigma_{33} > 0$

$$\frac{1}{S_{22}^T} (\sigma_{22} + \sigma_{33})^2 + \frac{1}{S_{23}^2} (\sigma_{23}^2 - \sigma_{22}\sigma_{33}) + \frac{1}{S_{12}^2} (\sigma_{12}^2 + \sigma_{13}^2) = 1 \quad (3.1)$$

Compressive Matrix Mode, $\sigma_{22} + \sigma_{33} < 0$

$$\frac{1}{S_{22}^C} \left[\left(\frac{S_{22}^C}{2S_{23}} \right)^2 - 1 \right] (\sigma_{22} + \sigma_{33}) + \frac{1}{4S_{23}^2} (\sigma_{22} + \sigma_{33})^2 + \frac{1}{S_{23}^2} (\sigma_{23}^2 - \sigma_{22}\sigma_{33}) + \frac{1}{S_{12}^2} (\sigma_{12}^2 + \sigma_{13}^2) = 1 \quad (3.2)$$

Tensile Fibre Mode, $\sigma_{11} > 0$

$$\left(\frac{\sigma_{11}}{S_{11}^T} \right)^2 + \frac{1}{S_{12}^2} (\sigma_{12}^2 + \sigma_{13}^2) = 1 \quad (3.3)$$

Compressive Fibre Mode, $\sigma_{11} < 0$

$$\sigma_{11} = -S_{11}^C \quad (3.4)$$

where $\sigma_{ij}, (i, j = 1, 2, 3)$ is the stress tensor and $S_{ij}, (i, j = 1, 2, 3)$ is the strength tensor. The superscripts *T* and *C* on the components of the strength tensor *S* denote material strength in tension and compression respectively. Since the material is insensitive to the sign of the shear stresses, the superscripts are omitted on the shear strengths S_{12}, S_{13} and S_{23} .

Some authors [35, 36] carried out a delamination initiation failure analysis using the Ye delamination initiation criteria [37]. Ye's stress-based strength criteria for delamination onset are shown below:

If $\sigma_{33} > 0$ then,

$$\left(\frac{\sigma_{33}}{S_{33}} \right)^2 + \left(\frac{\sigma_{13}}{S_{13}} \right)^2 + \left(\frac{\sigma_{23}}{S_{23}} \right)^2 = 1 \quad (3.5)$$

or if $\sigma_{33} < 0$

$$\left(\frac{\sigma_{13}}{S_{13}} \right)^2 + \left(\frac{\sigma_{23}}{S_{23}} \right)^2 = 1 \quad (3.6)$$

where the symbols are as before. The strength criteria required that the stress components be averaged over a critical distance, *C*, from the free edge because the strength properties were valid over a finite material volume and it was suggested that *C* be chosen equal to two ply thicknesses.

3.3 Non-linear shear behaviour

Experimental evidence has shown that in general, fibrous composites display a non-linear behaviour when loaded in shear but maintain essentially linear behaviour when loaded in longitudinal tension and longitudinal compression and mildly non-linear behaviour when loaded in transverse tension and transverse compression [28, 38, 39]. Hahn & Tsai [38] developed a non-linear stress/strain relationship using complementary energy density functions which resulted in a constitutive model that was linear in uni-axial loadings in longitudinal and transverse directions, but non-linear in shear. Their analysis was restricted to in-plane loading due to the lack of out-of-plane experimental data, but they stated that extension of their model to the three-dimensional case does not pose any conceptual difficulty, although the number of higher order constants to be determined increases greatly. A unique solution to their strain energy function was given as:

$$\varepsilon_{12} = \frac{\sigma_{12}}{G_{12}^0} + \alpha\sigma_{12}^3 \quad (3.7)$$

where α is a non-linear material parameter which has to be determined experimentally, ε_{12} is the in-plane engineering strain and G_{12}^0 is the initial lamina longitudinal-transverse shear modulus. Equation 3.7 only exists if,

$$\frac{d\varepsilon_{12}}{d\sigma_{12}} = \frac{1}{G_{12}^0} + 3\alpha\sigma_{12}^2 \neq 0 \quad (3.8)$$

A number of authors [19, 29, 30, 31, 40, 41] have used equation 3.7 to account for shear non-linearity in progressive damage modelling but their formulations were restricted to plane stress investigations. Shokrieh & Lessard [39] extended the non-linear shear behaviour to three dimensions by assuming that the normal-longitudinal shear modulus also varied in a non-linear manner similar to the longitudinal-transverse modulus given by equation 3.7, i.e.,

$$\varepsilon_{13} = \frac{\sigma_{13}}{G_{13}^0} + \alpha\sigma_{13}^3 \quad (3.9)$$

where ε_{13} is the normal-longitudinal engineering strain and G_{13}^0 is the initial lamina normal-longitudinal shear modulus.

3.4 Degradation Rules

When failure occurs in a composite material, the moduli of the material in the vicinity of the failed point decrease. The extent of this decrease has been the focus of several investigations. Nuismer & Tan [42] developed a constitutive relationship for a composite laminate containing cracks. Only in-plane material properties were considered, but it was shown that the extensional and shear stiffness decreased non-linearly as crack density increased. In a later paper, Tan & Nuismer [43] compared extensional and shear stiffness reduction to experimental results and good agreement was found. The paper also showed that the in-plane Poisson's ratio reduced with increasing crack density and good agreement with experiments

was also obtained. Lee et al. [44] developed an internal state variable approach for predicting stiffness reductions in fibrous laminated composites with matrix cracks and found similar reductions in stiffnesses as Nuismer & Tan [42] and Tan & Nuismer [43].

One of the simplest degradation methods is the complete ply failure approach used by Dato [45]. In this approach, it was assumed that the element had completely failed when the average stresses in that element satisfied any of the different failure criteria employed. The failed element was no longer able to sustain any load in any direction regardless of the failure mode and this was achieved by degrading all material properties of the failed element. This method was used by Chen & Lee [12] while analysing composite bolted laminates subjected to bending loads. More common methods which are more physically realistic than the complete ply failure approach degrade individual moduli depending on the failure mode detected and have been used by many researchers performing PDA [19, 29, 30, 40, 46, 47].

Once failure is detected the moduli associated with that failure mode have to be degraded. Different ways to do this (illustrated in figure 3.2) are: instantaneous unloading, gradual unloading and constant stress at ply failure. Instantaneous unloading has been achieved by setting the material property associated with that mode of failure to zero or some constant multiple of the original value. McLaughlin & Rosen [48] implemented instantaneous unloading by modifying parameters in their model to give essentially zero stress in the failed direction at large strain. Gradual unloading can be either linear or non-linear. Petit & Waddoups [49] applied a linear gradual unloading by giving the failed moduli a relatively high negative value. Nahas [24] used an exponential function, while Chang & Chang [46] used a Weibull distribution to simulate gradual unloading. An example of the constant stress at ply failure approach is the Hahn-Tsai method [50]. In this method, the failed lamina supported the load until total laminate failure occurred. Other post failure theories exist, but they can be considered as special cases as the ones discussed above and further information on these can be found in Nahas [24].

Many different researchers [12, 22, 29, 33, 41] have proposed different material property degradation rules when failure is detected at a material point and these are listed in Table 3.1. The list is not exhaustive, but it does illustrate that many different degradation rules have been used in both two-dimensional and three-dimensional analyses in the past. The numbers in each column represent the factor by which each material property was degraded after failure was detected.

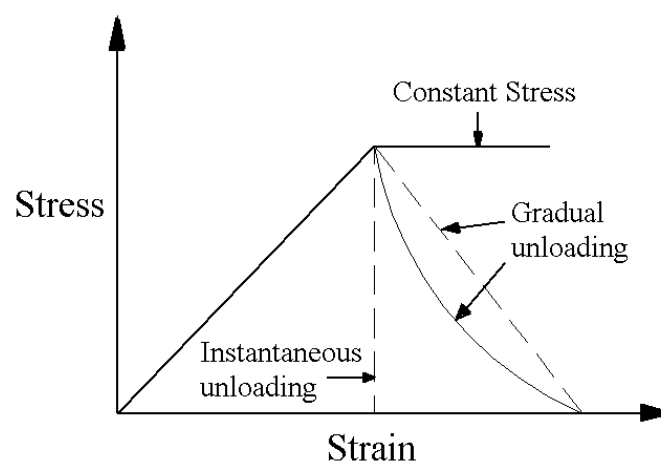


Figure 3.2 Different post-failure degradation methods [21]

Table 3.1 Material property degradation factors used by several authors

| | E ₁₁ | E ₂₂ | E ₃₃ | G ₁₂ | G ₂₃ | G ₁₃ | v ₁₂ | v ₂₃ | v ₁₃ |
|--|-----------------|-----------------|-----------------|-----------------|-----------------|-----------------|-----------------|-----------------|-----------------|
| (Camanho & Matthews 1999a) (3D) | | | | | | | | | |
| Tensile Matrix Mode | - | 0.2 | - | 0.2 | 0.2 | - | - | - | - |
| Tensile Fibre Mode | 0.07 | - | - | - | - | - | - | - | - |
| Compressive Matrix Mode | - | 0.4 | - | 0.4 | 0.4 | - | - | - | - |
| Compressive Fibre Mode | 0.14 | - | - | - | - | - | - | - | - |
| (Kermanidis et al. 2000) (3D) | | | | | | | | | |
| Tensile Matrix Mode | - | 0 | - | - | - | - | 0 | - | - |
| Tensile Fibre Mode | 0 | 0 | 0 | 0 | 0 | 0 | 0 | 0 | 0 |
| Compressive Matrix Mode | - | 0 | - | - | - | - | - | - | - |
| Compressive Fibre Mode | 0 | 0 | 0 | 0 | 0 | 0 | 0 | 0 | 0 |
| (Gamble, Pilling, & Wilson 1995) (3D) | | | | | | | | | |
| Fibre Failure | 0 | - | - | 0 | - | - | 0 | - | 0 |
| Matrix Failure | - | - | 0 | - | 0 | 0 | - | - | - |
| Matrix Splitting | - | 0 | - | 0 | - | - | - | 0 | - |
| (Chen & Lee 1995) (3D) | | | | | | | | | |
| Failure detected in any mode | 0 | 0 | 0 | 0 | 0 | 0 | 0 | 0 | 0 |
| (Lessard & Shokrieh 1995) (2D) | | | | | | | | | |
| Tensile Matrix Mode | - | 0 | * | 0 | * | * | 0 | * | * |
| Tensile Fibre Mode | 0 | 0 | * | 0 | * | * | 0 | * | * |
| Compressive Matrix Mode | - | 0 | * | 0 | * | * | 0 | * | * |
| Compressive Fibre Mode | 10 | 10 | * | 10 | * | * | 10 | * | * |
| (Kim, Hwang, & Kim 1998a) (2D) | | | | | | | | | |
| Tensile Matrix Mode | - | 0 | * | 0 | * | * | 0 | * | * |
| Tensile Fibre Mode | 0 | - | * | - | * | * | 0 | * | * |
| Compressive Matrix Mode | - | 0 | * | * | 0 | * | 0 | * | * |
| Compressive Fibre Mode | 0 | - | * | - | * | * | 0 | * | * |

- no reduction of moduli, * material property not applicable

In summary, it can be seen that there is a significant literature on the application of progressive damage mechanics using a stiffness reduction scheme to the composite bolted joint problem. However, many open questions remain. For example use of progressive damage in 3D models is still quite rare, and models which take into account both initiation and propagation of out-of-plane failure modes such as delamination are quite rudimentary. The influence of using different property degradation rules (e.g. those in Table 3.1) has not been assessed, and most models have convergence problems as damage progresses which precludes prediction of final failure loads. In short, a truly predictive progressive damage model that could predict the strength of a prospective joint in advance of testing with acceptable accuracy does not yet exist.

Section 4: Continuum Damage Mechanics

In this section, an overview is given of developments in Continuum Damage Mechanics (CDM). To the authors' knowledge CDM has not yet been used for modelling composite bolted joints, but it is intended in this project to apply existing CDM theories to bolted joints and also develop new CDM theories for the particular failure modes experienced in joints, so the topic is covered here.

As noted in Table 3.1, there are several variations in the literature of stiffness reduction schemes for modelling progressive damage in composites. Alternatively continuum damage mechanics methods have recently been developed to model some (though not all) composite failure modes in a mathematically more rigorous way. In the following section a brief review of existing CDM models is presented.

4.1 Allen's model [44, 51-53]

This CDM model uses internal state variables (ISV) to represent the average effects of local deformation due to the various modes of microcrack damage. The constitutive model for a local volume element may be written as:

$$\sigma_{ij_L} = Q_{ijkl} \{ \varepsilon_{kl} - \alpha_{kl} \}_L \quad (4.1)$$

In equation (4.1) σ_{ij_L} are the locally averaged components of stress, Q_{ijkl} are the ply-level reduced moduli, and ε_{kl_L} are the locally averaged components of strain. The internal state variables, α_{kl_L} , represent the local deformation effects of the various modes of damage. When the material is subjected to quasi-static (monotonic) loads, the incremental change of the internal state variable is assumed to be:

$$d\alpha_{kl_L} = \begin{cases} f(\varepsilon_{kl_L}, \beta, \gamma, \psi) & \text{if } \varepsilon_{kl_L} \geq \varepsilon_{kl_{crit}} \\ 0 & \text{if } \varepsilon_{kl_L} \leq \varepsilon_{kl_{crit}} \end{cases} \quad (4.2)$$

In equation (4.2) $\varepsilon_{kl_{crit}}$ is the critical tensile failure strain and β , γ , and ψ are scale factors that describe the load carrying capability of the material after the occurrence of mode I (opening mode) matrix cracking, fiber fracture, and mode II (shear mode) matrix cracking, respectively.

If the strains in a finite element are less than the critical strains, no damage exists and the internal state variables have a zero value. When the strains reach their critical value, the element is damaged and this damage is represented by an internal state variable whose value is proportional to the local strain.

When fiber fracture, mode II matrix cracking, or mode I matrix cracking is detected in a ply within an element, the relationship between the stresses and the strength parameters are given as follows:

$$\begin{aligned}\sigma_{11} &= \gamma S_{cr}^X \\ \sigma_{12} &= \psi S_{cr}^{XY} \\ \sigma_{22} &= \beta S_{cr}^Y\end{aligned}\quad (4.3)$$

In equation (4.3), S_{cr}^X , S_{cr}^{XY} and S_{cr}^Y are the lamina longitudinal, shear, and transverse critical strengths, respectively. The model has been used [51] to predict the damage initiation and growth in a center-notch tension specimen (figure 4.1).

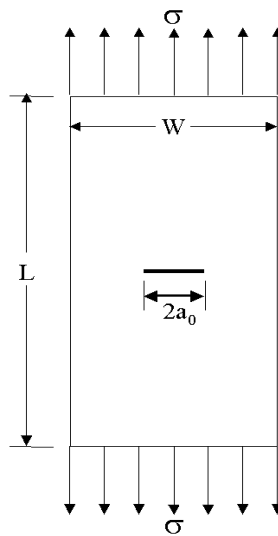


Figure 4.1 Centre notch tension specimen

4.2 Ladeveze's model [54-59]

The damage model developed in reference [54] is based on the hypothesis that laminated composites can be described by homogeneous layers (plies) together with ply interfaces. Three scalar damage variables are introduced. These variables are assumed to be constant throughout the thickness of the ply. The variables are: d_1 in the longitudinal direction, d_2 in the transverse direction, and d in shear.

The strain energy of an elementary ply is then written as:

$$E_d = \frac{1}{2} \left[\frac{\langle \sigma_{11} \rangle_+^2}{E_1^0(1-d_1)} + \frac{\langle \sigma_{11} \rangle_-^2}{E_1^0} - 2 \frac{\nu_{12}^0}{E_1^0} \sigma_{11} \sigma_{22} \right] + \frac{1}{2} \left[\frac{\langle \sigma_{22} \rangle_-^2}{E_2^0} + \frac{\langle \sigma_{22} \rangle_+^2}{E_2^0(1-d_2)} + \frac{\sigma_{12}^2}{(1-d)G_{12}^0} \right] \quad (4.4)$$

In equation (4.4), $\langle \cdot \rangle_+$ denotes positive part and $\langle \cdot \rangle_-$ indicates negative part, “0” indicates the initial value, and 1 and 2 are the fibre direction and the transverse direction, respectively.

Three strength variables (Y_1 , Y_2 , Y) are introduced which are thermodynamically associated with d_1 , d_2 and d , respectively:

$$Y_1 = \left. \frac{\partial [E_d]}{\partial d_1} \right|_{\sigma_{cons}} = \frac{1}{2} \frac{[\langle \sigma_{11}^2 \rangle_+]}{E_1^0(1-d_1)^2} \quad (4.5)$$

$$Y_2 = \left. \frac{\partial [E_d]}{\partial d_2} \right|_{\sigma_{cons}} = \frac{1}{2} \frac{[\langle \sigma_{22}^2 \rangle_+]}{E_2^0(1-d_2)^2} \quad (4.6)$$

$$Y = \left. \frac{\partial [E_d]}{\partial d} \right|_{\sigma_{cons}} = \frac{1}{2} \frac{[\sigma_{12}^2]}{G_{12}^0(1-d)^2} \quad (4.7)$$

Finally damage evolution laws can be established in terms of (Y_1 , Y_2 , Y).

4.3 Talreja’s CDM model [60]

Talreja presented a continuum damage model, where each damage entity is defined using two vectors: damage influence vector a_i and unit normal n_i (to damage entity surface). A damage entity tensor is then formed as follows:

$$d_{ij} = \int_S a_i n_j dS \quad (4.8)$$

For n distinct damage modes, the damage tensor is then defined as

$$D_{ij}^{\alpha} = \frac{1}{V} \sum_{k_{\alpha}} (d_{ij}^{\alpha}) k_{\alpha} \quad (4.9)$$

where $\alpha=1,2,\dots,n$, denote the damage modes, V is the volume of the RVE (representative volume element), and k_{α} represents the number of damage entities in the α th damage mode.

The following additional equations are also defined in the model.

$$d_{ij} = d_{ij}^1 + d_{ij}^2 \quad (4.10)$$

$$d_{ij}^1 = \int_S a n_i n_j dS \quad (4.11)$$

$$d_{ij}^2 = \int_S b m_i n_j dS \quad (4.12)$$

where a and b are the magnitudes of the normal and tangential projections, respectively, of vector a_i and vectors n_i and m_j are unit normal and tangential vectors, respectively.

The damage mode tensor D_{ij} is then written as:

$$D_{ij}^{\alpha} = D_{ij}^{1(\alpha)} + D_{ij}^{2(\alpha)} \quad (4.13)$$

$$D_{ij}^{1(\alpha)} = \frac{1}{V} \sum_{k_{\alpha}} (d_{ij}^1) k_{\alpha} \quad (4.14)$$

$$D_{ij}^{2(\alpha)} = \frac{1}{V} \sum_{k_{\alpha}} (d_{ij}^2) k_{\alpha} \quad (4.15)$$

4.4 Plasticity based CDM model [61-62]

There are two well known anisotropic yield criteria: Hill's yield criterion and Hoffman's criterion. Both yield criteria are represented by a yield function that bounds all states of stress in a material point. In the former case, the yield function is described by six independent material parameters representing the three tensile strengths and the three shear strengths of the material. For the description of the Hoffman's yield surface, nine independent material parameters are necessary which represent the three tensile strengths, the three compressive strengths and the three shear strengths of the material.

The Hoffman yield criterion can be written in the following manner:

$$\frac{1}{2} \sigma^T P \sigma + \sigma^T q - \bar{\sigma}_0^2 \quad (4.16)$$

where $\sigma = (\bar{\sigma}_{11}, \bar{\sigma}_{22}, \bar{\sigma}_{33}, \bar{\sigma}_{12}, \bar{\sigma}_{23}, \bar{\sigma}_{31})$.

In the above equation the stress $\bar{\sigma}_0$ represents the equivalent stress. The mathematical expressions for the mapping matrix P, and the mapping vector q can be found in reference [61].

The above equation is then re-written in a strain based format so that an expression for the damage initiation surface can be obtained. The model has been applied [62] to predict the effect of transverse cracking on the stiffness of the material in a laminated composite plate with a central circular hole (figure 4.2).

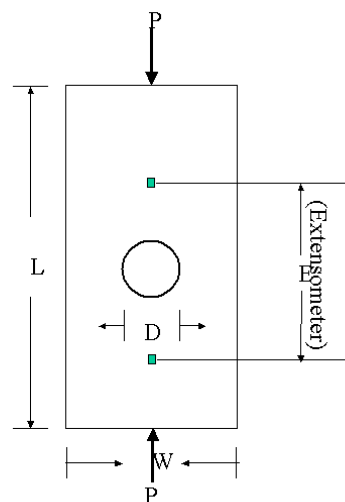


Figure 4.2 Laminated composite plate with a central circular hole

In summary, four of the most important CDM models available in the literature have been reviewed. Based on the review, it can be concluded that CDM methods have been applied for predicting damage in center-notch specimens and open-hole specimens. However, at present, there are no CDM methodologies for predicting damage initiation and propagation in composite bolted joints.

Section 5: Conclusions

Based on the reviews made in the previous three sections, the following general conclusions and recommendations can be made.

- Three-dimensional progressive failure analysis of composite bolted joints is still a complex task. Establishing an accurate material property degradation scheme will need careful observation of the damage initiation and propagation processes in the experiments to be performed in WP 3 of this project.
- From this, a three-dimensional progressive failure methodology (**Damage Model I** in the proposal) for analysis of composite bolted joints will be developed and implemented in the finite element program ABAQUS. A suitable material property degradation scheme will be established for this purpose.
- An internal state variable based continuum damage mechanics model for analysis of composite bolted joints will be developed. As outlined in the proposal, this CDM model will be completed in two phases. In Phase 1, tensile damage modes such as Mode I (opening mode) matrix cracking, fibre breakage, and Mode II (shear mode) matrix cracking will be considered. Damage growth laws for all these damage modes will be derived and implemented in ABAQUS user subroutines (**Damage Model II(a)**). In Phase 2, compressive (bearing) failure will be included in the damage model. Damage growth laws for failure modes such as matrix crushing and fibre kinking will be derived. The damage growth laws derived in Phase 1 and Phase 2 will then be integrated to obtain the CDM-based damage model for composite joints (**Damage Model II(b)**).
- The models II(a) and II(b) will be 3-D in nature containing all the six stresses and strains.

Acknowledgements

The authors would like to gratefully acknowledge Enterprise Ireland and the Irish Research Council for Science, Engineering and Technology for funding this work.

References

1. Oplinger, D.W., 1996 "AGARD conference on Bolted/bonded joints in polymeric composites", Florence, Italy, Paper 1.
2. Camanho, P.P. & Matthews, F.L., 1997. "Stress analysis and Strength prediction of Mechanical Fastened joints in FRP: a Review" Composites Part A, 28, 529-547.
3. Hart-Smith, L.J., 1978. "Mechanical-Fastened Joints for Advanced Composites - Phenomenological Considerations and Simple Analysis", Plenum Press, New York, pp. 543-574.
4. TANGO 1998, "Technology Application to the Near-Term Business Goals and Objectives of the Aerospace Industry". Contract No. G4RD-CT-2000-00241, <http://www.tangoecproject.com/>.
5. M.A. McCarthy, 2001, "BOJCAS: Bolted Joints in Composite Aircraft Structures", *Air and Space Europe*, No. 3/4, Vol. 3, pp. 139-142.
6. Starikov, R. & Schon, J., 2001. "Quasi-Static Behaviour of Composite Joints with Protruding-head Bolts", *Composite Structures*, 51, 411-425.
7. Camanho, P.P., Bowron, S. & Matthews, F.L., 1998. "Failure Mechanisms in bolted CFRP", *Journal of reinforced plastics and composite*, 17(3), 205-233.
8. Wang, H., Hung, C. & Chang, F.K., 1996. "Bearing Failure of Bolted Composites Joints. Part I: Experimental Characterisation", *Journal of Composite Materials*, 30(12), 1285-1313.
9. Cooper, C. & Turvey, G.J., 1995. "Effects of Joint Geometry and Bolt Torque on the Structural Performance of Single Bolt Tension Joints in Pultruded GRP Sheet Material" *Composite Structures*, 32, 217-226.
10. Hart-Smith, L.J., 1976. Bolted Joints in Graphite-Epoxy Composites, NASA Contractor Report, NASA CR-1444899.
11. Kretsis, G. & Matthews, F.L., 1985. "The Strength of Bolted Joints in Glass Fibre/Epoxy laminates", *Composites*, 16, 92-105.
12. Chen, W.H. & Lee, S.S., 1995. "Numerical and Experimental Failure Analysis of Composite Laminates with Bolted Joints under Bending Loads", *Journal of Composite Materials*, 29(1), 15-36.
13. Lawlor, V.P., Stanley, W.F. & McCarthy, M.A., 2002. "Characterisation of Damage Development in Single Shear Bolted Composite Joints", *Plastics, Rubber and Composites*, 31(3), 126-133.
14. Whitney, J.M. & Nuismer, R.J., 1974. "Stress Fracture Criteria for Laminated Composites Containing Stress Concentrations", *Journal of Composite Materials*, 8, 235-265.

15. [Crews, J.H. & Naik, R.A., 1987. "Bearing Bypass Loading on Bolted Composite Joints", National Aeronautics and Space Administration, Washington, D.C., NASA TM 89153.](#)
16. [DiNicola, A. J. & Fantle, S.L., 1993. "Bearing strength of clearance fit fastener holes in toughened graphite/epoxy laminates", Composite Materials: Testing and Design, ASTM STP 1206, 11, 220-237.](#)
17. [Friberg, M. & Nyman, T., 2000. "Interlaminar Stresses in Notched and Un-notched Composite Laminates", Journal of Reinforced Plastics and Composites, 19, 34-57.](#)
18. [Chiang, Y.J. & Rowlands, R.E., 1991. "Finite Element Analysis of Mixed-Mode Fracture of Bolted Composite Joints", Journal of Reinforced Plastics and Composites, 13\(4\), 227-235.](#)
19. [Dano, M.L., Gendron, D. & Picard, A., 2000. "Stress and Failure Analysis of Mechanically Fastened Joints in Composite Laminates", Composite Structures, 50, 287-296.](#)
20. [Lessard, B.L., 1989. "Compression Failure in Laminated Composites Containing an Open Hole". Ph.D. Thesis, Stanford University.](#)
21. [Sleight, D.W., 1999. "Progressive Failure Analysis Methodology for Laminated Composite Structures", Washington, DC 20546-0001, NASA/TP-19999-209107.](#)
22. [Camanho, P.P. & Matthews, F.L., 1999. "A Progressive Damage Model for Mechanically Fastened Joints in Composite Laminates", Journal of Composite Materials, 33\(24\), 2248-2280.](#)
23. [Hung, C.L. & Chang, F.K., 1996. "Strength Envelope of Bolted Composite Joints under Bypass Loads", Journal of Composite Materials, 30\(12\), 1402-1435.](#)
24. [Nahas, M.N., 1986. "Survey of Failure and Post-Failure Theories of Laminated Fibre-Reinforced Composites", Journal of Composites Technology and Research, 8\(4\), 138-153.](#)
25. [Hill, R., 1950. "The Mathematical Theory of Plasticity", Oxford University Press.](#)
26. [Azzi, V.D. & Tsai, S.W., 1965. "Anisotropic Strength of Composites", Experimental Mechanics, 5, 282 – 288.](#)
27. [Tsai, S.W. & Wu, E.M., 1971. "A General Theory of Strength for Anisotropic Material", Journal of Composite Materials, 5, 58 – 80.](#)
28. [Daniel, I.M. & Ishai, O., 1994. "Engineering Mechanics of Composite Materials". Oxford University Press.](#)
29. [Lessard, L.B. & Shokrieh, M.M., 1995. "Two-Dimensional Modelling of Composite Pinned-Joint Failure", Journal of Composite Materials, 29\(5\), 671-697.](#)
30. [Chang, F.K. & Chang, K.Y., 1987. "Post-Failure Analysis of Bolted Composite Joints in Tension or Shear-Out Mode Failure", Journal of Composite Materials, 21, 809-833.](#)

31. Chang, F.K., Scott, R.A. & Springer, G.S., 1984. ["Failure Strength of Nonlinearly Elastic Composite Laminates Containing a Pin Loaded Hole"](#), [Journal of Composite Materials](#), 18, 464-477.
32. Hung, C.L. & Chang, F.K., 1996. ["Bearing Failure of Bolted Composite Joints. Part II: Model and Verification"](#), [Journal of Composite Materials](#), 30(12), 1359-1400.
33. Kermanidis, T., Labeas, G., Tserpes, K.I. & Pantelakis, S., 2000. ["Finite Element Modelling of Damage Accumulation in Bolted Composite Joints under Incremental Tensile Loading"](#), [European Congress on Computational Methods in Applied Sciences and Engineering](#), ed., ECCOMAS 2000, Barcelona.
34. Hashin, Z., 1980. ["Failure Criteria for Unidirectional Fiber Composites"](#), [Journal of Applied Mechanics](#), 47, 329-334.
35. Camanho, P.P. & Matthews, F.L., 1999. ["Delamination Onset Prediction in Mechanically Fastened Joints in Composite Laminates"](#), [Journal of Composite Materials](#), 33(10), 906-927.
36. Chen, W.H., Lee, S.S. & Yeh, J.T., 1995. ["Three-dimensional contact stress analysis of a composite laminate with bolted joint"](#), [Composite Structures](#), 30, 287-297.
37. Ye, L., 1988. ["Role of Matrix Resin in Delamination Onset and Growth in Composite Laminates"](#), [Composites Science and Technology](#), 33, 257-277.
38. Hahn, H.T. & Tsai, S.W., 1973. ["Non-linear Elastic Behaviour of Unidirectional Composite Laminate"](#), [Journal of Composite Materials](#), 7, 102-118.
39. Shokrieh, M.M. & Lessard, B.L., 1996. ["Effects of Material Nonlinearity on the Three-Dimensional Stress State of Pin-Loaded Composite Laminates"](#), [Journal of Composite Materials](#), 30(7), 839-861.
40. Chang, F.K. & Lessard, L.B., 1991. ["Damage Tolerance of Laminated Composites Containing an Open Hole and Subjected to Compressive Loadings: Part I – Analysis"](#) [Journal of Composite Materials](#), 25, 2-43.
41. Kim, S.J., Hwang, J.S. & Kim, J.H., 1998. ["Progressive Failure analysis of Pin-Loaded Laminated Composites using Penalty Finite Element Method"](#), [AIAA](#), 36(1), 75-80.
42. Nuismer, R.J. & Tan, S.C., 1988. ["Constitutive Relations of a Cracked Composite Lamina"](#), [Journal of Composite Materials](#), 22, 306-321.
43. Tan, S.C. & Nuismer, R.J., 1989. ["A Theory for Progressive Matrix Cracking in Composite Laminates"](#), [Journal of Composite Materials](#), 23, 1029-1047.
44. Lee, J.W., Allen, D.H. & Harris, C. E., 1989. ["Internal State Variable Approach for Predicting Stiffness Reductions in Fibrous Laminated Composites with Matrix Cracks"](#), [Journal of Composite Materials](#), 23, 1273-1291.

45. Dato, M.H., 1991. NY: Elsevier Science Publishing Co., Inc., New York.
46. Chang, F.K. & Chang, K.Y., 1987. "[A Progressive Damage Model for Laminated Composites Containing Stress Concentrations](#)", *Journal of Composite Materials*, 21, 834-855.
47. Papanikos, P., Tserpes, K.I. & Pantelakis, S., 2002. "Modelling of Fatigue Damage Progression and Life of Carbon Fibre-Reinforced Plastics Laminates", *Fatigue Fract. Engng. Mater. Struct.*, 25, 1-11.
48. McLaughlin, P.V. & Rosen, B.W., 1972. "Combined Stress Effects Upon Failure of Fibre Composites", Blue Bell, PA, TFR/7404/1112.
49. Petit, P.H. & Waddoups, M.E., 1969. "[A Method of Predicting the Non-Linear Behaviour of Laminated Composites](#)", *Journal of Composite Materials*, 3, 2-19.
50. Hahn, H.T., & Tsai, S.W., 1974. "[On the Behaviour of Composite Laminates After Initial Failures](#)", *Journal of Composite Materials*, 3, 2-19
51. Coats, T.W. and Harris, C.E., 1998. "A Progressive Damage Methodology for Residual Strength Predictions of Notched Composite Panels", National Aeronautics and Space Administration Technical Memorandum 1998-207646.
52. Coats, T.W. and Harris, C.E., 1995. "[Experimental Verification of a Progressive Damage Model for IM7/5260 Laminates Subjected to Tension-Tension Fatigue](#)," *J. of Composite Materials*, 29, 280-305.
53. Lo, D.C., Coats, T.W., Harris, C.E., and Allen, D.H., 1996. "[Progressive Damage Analysis of Laminated Composite \(PDALC\) \(A Computational Model Implemented in the NASA COMET Finite Element Code\)](#)," National Aeronautics and Space Administration Technical Memorandum 4724.
54. Gasser, A., Ladeveze, P. and Peres, P., 1998. "[Damage modelling for a laminated ceramic composite](#)", *Materials Science and Engineering A*, 250, 249-255.
55. Ladeveze, P. and Lubineau, G., 2001. "[On a damage mesomodel for laminates: micro-meso relationships, possibilities and limits](#)". *Composites Science and Technology*, 61, 2149-2158.
56. Ladeveze, P., Allix, O., Deü, J. and Lévêque, D., 2000. "A mesomodel for localisation and damage computation in laminates", *Computer Methods in Applied Mechanics and Engineering*, 183, 105-122.
57. Allix, O., Ladevéze, P., and Corigliano, A., 1995., "[Damage analysis of interlaminar fracture specimens](#)", *Composite Structures*, 31, 61-74.
58. Ladevèze, P. and Lubineau, G., 2003. "[On a damage mesomodel for laminates: micromechanics basis and improvement](#)", *Mechanics of Materials*, 35, 763-775.

59. [Ladeveze, P. and LeDantec, E., 1992. "Damage modelling of the elementary ply for laminated composites", Composites Science and Technology, 43, 257-267.](#)
60. [Kumar, R.S. and Talreja, R., 2003. "A continuum damage model for linear viscoelastic composite materials", Mechanics of Materials, 35, 463-480.](#)
61. [Hashagen, F. and de Borst, R., 2001. "Enhancement of the Hoffman yield criterion with an anisotropic hardening model", Computers & Structures, 79, 637-651.](#)
62. [Schipperen, J.H.A., 2001. "An anisotropic damage model for the description of transverse matrix cracking in a graphite–epoxy laminate", Composite Structures, 53, 295-299.](#)